Title: Volume change behaviour of a cement kiln dust

Author 1

Yahya Hamza Karagoly

Civil Engineering Department, Faculty of Engineering, University of Babylon, P.O Box 4, Al Hillah, Babil, Iraq 51002

Author 2

Osama Mahdi Al-Hussaini

Department of Civil Engineering, University of Kufa, P.O Box 21, Kufa, Najaf, Iraq 540011

Author 3

Snehasis Tripathy

Professor in Civil Engineering, School of Engineering, Cardiff University, Queen's Buildings, West Grove, Newport Road, Cardiff CF243AA UK

https://orcid.org/0000-0003-1632-7668

Author 4

Peter John Cleall

Professor in Civil Engineering, School of Engineering, Cardiff University, Queen's Buildings, West Grove, Newport Road, Cardiff CF243AA UK

https://orcid.org/0000-0002-4005-5319

Corresponding author:

Snehasis Tripathy

Professor in Civil Engineering, School of Engineering, Cardiff University

Queen's Buildings, West Grove, Newport Road

Cardiff CF243AA UK

TripathyS@cardiff.ac.uk

Volume change behaviour of a cement kiln dust

Yahya Hamza Karagoly, Osama Mahdi Al-Hussaini, Snehasis Tripathy, Peter John Cleall

Abstract

Industrial wastes are damage to the environment and pose threat to public health. Utilization of industrial wastes becomes inevitable if a circular economy needs to be achieved. Cement kiln dust is a potential engineering material that may be used in many civil engineering works. The volume change behaviour of a cement kiln dust is reported in this paper. One-dimensional swelling and compression tests were carried out on cement kiln dust specimens to derive the compressibility parameters and coefficient of permeability. A cyclic wet-freeze-thaw-dry test was carried out to study the volume change of the material upon exposed to various seasonal climatic processes under a low surcharge pressure. The experimental results showed that cement kiln dusts may exhibit swelling under light loads. The correlations between plasticity properties and compressibility parameters that are applicable for fine grained soils, were found to overestimate the parameters of the cement kiln dust. The magnitudes of frost heave and thaw settlement were found to be significant, with an uprising type of movement accompanied by strain accumulation when the material was taken through several wet-freeze-thaw-dry cycles.

Keywords: Volume change, Oedometer tests, Compressibility, industrial waste, cement kiln dust, seasonal climatic processes

Introduction

Population growth alongside increasing urbanisation and rising standards of living have led to generation of a large quantity and variety of solid wastes by industrial, mining, domestic and agricultural activities. Some of the industrial wastes generated are steel slags, plastics, glass, fly ash, cement kiln dust (CKD), silica fume, and mine tailings (Environmental Agency 2021). The use of industrial waste increases the sustainability of industrial processes. Geotechnical and geoenvironmental engineering applications of various wastes have been considered where the native soils do not meet the design criteria in terms of compressibility, shear strength, ion retention, and permeability, among these are fly ash and cement kiln dust (Miller and Azad 2000; Button 2003; Adaska and Taubert 2008; Peethamparan et al. 2008; Sridharan and Prakash 2009).

Cement kiln dust (CKD) is a by-product of the Portland cement manufacturing process. The global cement production is estimated to about 4.0 billion tonnes per year (Heincke et al. 2023). The worldwide CKD generation is estimated to be about 420 – 560 million tonnes during the year 2009 (Kunal et al. 2012). This suggests that the amount of CKD produced annually is about 10 to 14% of the amount of cement produced. The material is a fine powder with a wide range of particle sizes and poses storage problems, health hazards, and is a potential pollution source (Baghdadi et al. 1995).

Adaska and Taubert (2008) stated that CKD sent to landfill is decreasing in the United States. This is because a large quantity of CKDs is used in beneficial applications, such as soil stabilization, stabilization/solidification of waste materials, cement additive/blending and mine reclamation. In the United Kingdom, no CKD has been sent to landfill since 2012 (Department for Business and Trade 2023). The CKDs are either returned to the kilns as feed stock or are utilized in a number of secondary applications, such as in agriculture as liming agent, soil

stabilization, concrete mix, chemical treatment and ceramic and brick manufacturing. Several other studies reported the use of CKDs alone or as a mixture with soils in various applications including the stabilization of weak soils, construction of hydraulic barrier systems, pavements, low-strength backfill, engineered barriers for landfill liners, mine reclamation, and in agriculture (Baghdadi and Rahman 1990; USEPA 1998; ASTM 2015). In most of the geotechnical engineering applications the admixture soils are used in compacted form above the groundwater table. Therefore, the materials often are in unsaturated state.

Studies in the past have shown that the collapse potential and compressibility of soils decreased upon using CKD as a stabiliser additive (Miller et al. 1997). Similarly, an addition of CKD was found to decrease the swelling potential of expansive soils (Parsons et al. 2004). Differences in the characteristics of already landfilled and fresh CKDs have been reported (Sreekrishnavilasam and Santagata 2006). This suggests that it would be necessary to determine properties of CKDs prior to their use in various engineering works.

Compacted materials may undergo numerous cycles of wetting, drying, freezing and thawing processes during their use in many civil engineering applications (roadways, railway formations, backfill and foundations). In temperate regions of the world, the materials are often subjected to drying and wetting processes, whereas in the cold regions, freezing and thawing processes are more common. In certain parts of the world, it may be expected that all these processes are prevalent. Considerable field and laboratory research works have been aimed at understanding the effects of cyclic wetting-drying (Tripathy et al. 2002) and cyclic freezing-thawing on the volume change behaviour of soils (Chamberlain and Gow 1979; Konrad 1989; Viklander 1998a,b; Qi et al. 2008; Hui and Ping 2009; Wang et al. 2016). The studies have shown that soils tend to reach an equilibrium in terms of the strain after several cycles of wetting-drying and freezing-thawing.

Determination of the basic properties and characteristics of materials are required to understand how the materials would respond to a variety of stress and environmental loading conditions. The engineering properties that are usually determined include the volume change (swelling/heave and settlement), permeability and shear strength. Studies on the volume change behaviour of compacted materials are beneficial which provide crucial information on the suitability of the materials for various engineering applications. Consolidation tests on initially saturated slurried materials provide information on the volume change and permeability for a wide range of applied stresses.

The presence of significant percentages of fine-size fractions and the chemical composition of CKD may influence the volume change behaviour of the material. In particular, the interaction of CKD with water and the formation of various minerals and hydroxides may contribute to the engineering properties. Volumetric changes of CKD may cause undesirable effects on the stability of engineering structures. Therefore, studies on the volume change behaviour of CKDs may lead to better understanding of their suitability as soil stabilizers. A detailed review of the literature indicated volume change behaviour of CKD alone in response to mechanical loading and seasonal climatic processes have not yet been explored in detail. The objectives of this paper are: (1) To study the one-dimensional swelling and compression behaviour of a CKD at various applied pressures so as to derive the relevant compressibility parameters and (2) To study the volume change behaviour of compacted CKD with an increasing number of freeze-thaw-dry-wet cycles.

Materials and methods

The CKD used in this study was supplied by a local cement company in Wales, UK. Table 1 presents the properties of the CKD used. The CKD contained 71% silt-size particles and 29% of particles were finer than clay-size (Fig. 1).

The liquid and plastic limits tests were performed after 1, 3, 7, 14 and 28 days of curing. The curing times were considered to study the effect of minerals and hydroxides that are formed due to the interaction of CKD with water (Peethamparan et al. 2008) on the plasticity properties. Figure 2 shows the curing time versus liquid limit, plastic limit and plasticity index of the CKD used. Minor variations of liquid and plastic limits were noted (about 2%) for the curing times considered which indicate that the impact of curing time on the Atterberg limits of the CKD was not very significant. This is possibly because at high water content of the CKD-water mixture (> liquid limit), the calcium-silicate-hydrate (C-S-H) gel bonding formed (Peethamparan et al. 2008) was weaker. Additionally, remixing of the CKD-water mixture prior to the tests eliminated the strength gain during the curing period. Light compaction test (BS 1377 1990a) results showed that the degree of saturation corresponding to the maximum dry unit weight and optimum water content was about 95% (Fig. 3).

The exchangeable cations in the CKD (Table 1) were mainly Ca^{2+} (60.12 meq/100g) with varying percentages of K^{+}, Na^{+} and Mg^{2+}. The specific surface of the CKD (0.58 m^2/g) was found to be within the range of values reported for several CKDs (0.19 - 0.65 m^2/g) (Mackie et al. 2010).

Chemical analysis of the CKD was performed using the X-ray fluorescence spectroscopy. The results (Table 2) show that the CKD was mainly composed of the oxides of calcium, silica and aluminium and the loss on ignition (LOI) was found to be 33.8%. The composition of the CKD is similar to the cement kiln raw feed; however, the amounts of alkalis (Na_2O and K_2O) and sulphate (SO_3) are usually considerably higher in the dust (Ravindrarajah 1982). The quantities of free lime (CaO) and alkalis may vary widely between CKDs. The exposure of stockpiled CKD to water can lead to the hydration of free lime with a decrease in free lime content and an increase in loss on ignition value (Button 2003).

The X-ray diffraction test and semi-quantitative analyses were undertaken to determine type and amounts of various minerals present in the CKD (Fig. 4). The dominant mineral in the CKD was found to be Calcite, $CaCO_3$ (85%). The CKD was also comprised Quartz, SiO_2 (12%) and traces of Gypsum, Kaolinite and Anhydrite. The microscopic appearance of the CKD powder (Fig. 5) predominantly composed of clusters (agglomerates) of particles with poorly defined shapes.

Experimental methods

Oedometer tests

One-dimensional compression test was carried out on an initially saturated slurried CKD specimen (70 mm dia and 15 mm), denoted as specimen SS. The specimen was prepared at an initial water content of 1.2 times the liquid limit of the CKD. The specimen was step-wise loaded to 800 kPa and then unloaded. A manual loading oedometer with a maximum loading capacity of 1000 kPa was used this purpose. One-dimensional swelling and compression tests (BS 1377 1990c) were conducted on statically compacted CKD specimens. The compacted CKD specimens (70 mm dia and 15 mm) were prepared at dry unit weight and water content of 14.83 kN/m^3 and 27.3% respectively. The chosen compaction conditions were similar to the optimum conditions of the CKD. Compacted unsaturated specimens were firstly inundated with water under an applied pressure of either 2 kPa (specimen CS-2 kPa) or 25 kPa (specimen CS-25 kPa). Once the swelling strains attained an equilibrium, the specimens were loaded in a step-wise manner up to a vertical pressure of 1600 kPa and then unloaded. The choice of initial pressures at the time of inundation with water was based on the potential engineering applications of CKDs (e.g., as landfill cover, and as subgrade materials) and the possible average in-situ overburden pressure. Similar applied pressures have been considered by Al-Rawas et al. (2002). A compacted specimen (specimen CS-CV, where CS stands for

compacted-saturated and CV for constant volume) was hydrated hydrated with water at constant volume condition to determine the swelling pressure. Specimens CS-2 kPa, CS-25 kPa and CV were tested in an automatic oedometer with a maximum loading capacity of 1800 kPa.

Cyclic freeze-thaw-dry-wet test

The laboratory test setup used to perform the cyclic freeze-thaw-wet-dry tests (Tripathy et al. 2020) is shown in Fig. 6. Using the test set up, it is not required to dismantle a specimen at any stage of the test while the specimen is taken through cycles of wetting, freezing, thawing, and drying. The test set up enabled applying predetermined temperature boundary conditions at the top of a specimen (diameter = 103.3 mm and height = 65 mm) and measuring vertical deformation and changes in the temperature at various predetermined heights of the specimen.

The test setup consists of a cylindrical polyvinyl chloride (PVC) interior and exterior mould assembly, a vortex tube that can supply temperature controlled hot or cold air to a top cooling/heating chamber, linear variable displacement transformers (LVDTs) to measure vertical deformation (measurement range = 50 mm, linearity = 0.2%, resolution = 0.3μm, and operating temperature range = - 40 to +120 °C), six thermocouples (RS Pro K Type thermocouples; measurement range = – 50 to + 250 °C, response time = 0.7 seconds, and accuracy = ±1.5 °C); two within the heating/cooling chamber to monitor temperature at the top of the specimen and four at predetermined length of the specimen, a porous stone, a water reservoir, a thermal insulation sheath (30 mm-thick rock-wool layer covered with a 3.7 mm thick reflective foil), an air supply system, and a data acquisition system. The PVC mould assembly comprises a single-flanged exterior mould and a step-flanged interior mould. The exterior mould is attached to a PVC base plate. An acrylic hollow cylinder-stand with a perforated acrylic disc at the top is placed within the exterior mould in order to create a water

reservoir below a porous stone, which in turn is placed on a perforated acrylic disc. The interior mould, with the thermocouples attached to the inner face, is made to rest on the perforated acrylic disc. The annular space between the interior and exterior moulds accommodates the ultrathin wires of the thermocouples. The specimen is placed on the porous stone, whereas the cooling/heating chamber is placed above the specimens during the tests. The LVDT holders are attached to a horizontal frame (not shown) which in turn is positioned directly on top of the device. The LVDTs on the heating/cooling chamber and on the flange of the interior mould measured the vertical deformation of the specimen and the interior mould.

The vortex tube is connected to the top cooling/heating chamber, which is a composite cylinder with a stainless-steel side and a 1.8 mm thick copper base. A 12.5 mm-thick PTFE disc with six air vents, each 10 mm in diameter, is attached firmly to the top open end of the stainless cylinder. Compressed air (7-bar; 1 bar = 100 kPa) is fed transversely into the generation chamber of the vortex tube that is made to spin by a generator. The air moves down the long tube in which hot air separates outwards and towards the wall of the tube due to the inertia of motion, whereas the cold air is pushed to the centre of the tube. A percentage of the hot air is made to exit (hot end), whereas the remaining air flows towards opposite end (cold end). The cold air supplied by the vortex tube can be used to apply freezing temperature at the top of the specimen, whereas the hot air can be used during the drying cycle. The pressurised air (cold or hot) exits the top chamber via the air vents.

The duration of each simulated ‘season’ can have a significant impact on the volume change behaviour of various materials. The experimental program adopted in this study does not attempt replicate the real length of annual seasons, with only laboratory-scale testing of the CKD with assumed temperature and hydraulic boundary conditions for predetermined periods of testing. The test was carried out at an applied vertical pressure of 2.0 kPa on the specimen (i.e., the self-weight of the heating/cooling chamber and the attached accessories).

A compacted specimen with initial water content of 24.2% and dry unit weight of 12.55 kN/m^3 was tested in the device. The compaction conditions of the specimen correspond to the dry side of the optimum conditions. The specimen was wetted at ambient laboratory temperature of 21 ± 2 °C. The supply of water to the water reservoir was from an external water reservoir (item 1 in Fig. 6). The freezing process followed the wetting process. The temperature at the top of the specimens was lowered down to -19 ± 0.5 °C and maintained for 24 hours, whereas the thawing process occurred at the ambient laboratory temperature.

When particulate systems (in this case, compacted CKD-water mixture) containing fine fractions are frozen from one side with an access to water on the opposite side, frost heave continues to develop due to two simultaneous processes. Firstly, the pore water freezes causing heave and secondly, water is cryogenically drawn from both unfrozen parts of the system and the external water source to the segregation freezing front, leading to the formation ice lenses within the particulate system causing further heave (Konrad 1989). In the current study, for comparing the magnitude of frost heave in various freezing cycles, the freezing process was therefore terminated after 24 hours in each cycle.

During the drying process, the temperature at the top of the specimen was maintained at 52 ± 1.5 °C. Each cycle comprised wetting, freezing, thawing and drying processes. The specimen was taken through several such cycles. Except for the freezing process in each cycle which was for 24 hr, in all other processes a change in the process was made when the vertical deformation of the specimen attained an equilibrium. During the initial phase of the investigation, the water contents of the materials at the end of drying cycles were determined. The results showed that the materials underwent partial drying process with water content at the end of each drying cycle was greater than the initial water content of the compacted specimen by about 1%. After termination of the drying stage and before starting the next wetting stage, a duration of 24 hours was allowed for the temperature in the specimen to attain

the room temperature. No water was supplied to the specimen during the drying process. During the wetting process, the water level was kept at the top of the specimen, whereas during freezing and thawing stages the water table was kept at the bottom of the specimen.

The frictional resistance between the specimen and the inner surface of the PVC mould was minimised by using silicon grease. However, during a freezing cycle, a subzero temperature at the top of the specimen caused ice formation at and near the top end of the specimen. The top end of the specimen remained adhered to the wall of the specimen mould (adfreezing effect) (Eigenbrod 1996) by the ice formed which in turn did not allow the expansion of the specimens to occur in an upward direction due to the development of side friction. The expansion of the specimen occurred towards the bottom end (in the direction of least resistance) thereby lifting the interior mould upwards.

Results and discussion

Swelling strain and swelling pressure

Figure 7 presents the elapsed time versus swelling strain results of the compacted CKD specimens (CS–2 kPa and CS–25 kPa). The swelling strains were calculated based on the change in heights and the initial height of the specimens prior to the saturation process. Figure 8 presents the development of swelling pressure with elapsed time during the saturation process of the compacted CKD specimen (CS–CV). The test was conducted in constant volume condition for a duration of about 24 days.

The effect of an applied pressure during inundation is found to be distinct on the swelling strain. An increase in the swelling strain was rapid during the initial stage for the specimen with an applied pressure of 2 kPa as compared to the specimen with an applied pressure of 25 kPa. The swelling strains attained equilibrium (18.8 and 1.47% at applied pressures of 2 and 25 kPa respectively) in both cases in about 23 days and 16 days under 2 kPa

and 25 kPa, respectively. The swelling pressure was found to increase and attained a maximum value of about 67 kPa at the end of 15 days and then decreased to reach a near constant value of about 60 kPa (Fig. 8).

The interaction of CKD with water is complex due to the presence of alumina (Al_2O_3), silica (SiO_2), calcium oxide (CaO), alkalis (Na_2O and K_2O) and sulfate (SO_3). Peethamparan et al. (2008) stated that CKDs with high contents of free-lime upon hydration produced significant amounts of calcium hydroxide ($Ca(OH)_2$), calcium–silicate-hydrate (C-S-H), gypsum, ettringite, and syngenite. Ramachandran et al. (1964) stated that hydration of calcium oxide (CaO) is associated with an increase in the crystal volume, and a decrease in the pore volume and size. Liyanaga and Gamage (2021) stated that volume expansion due to hydration of CaO is due to formation and lengthening of calcium hydroxide crystals around the hydrating CaO. Thus, an increase in the volume and the swelling pressure exhibited of the CKD upon exposed to water can be attributed to the chemical reaction between CaO and water. A reduction in swelling strain due to an increase in the surcharge pressure suggests that the lengthening of calcium hydroxide crystal is countered by the applied stress. Additionally, the C-S-H-gel system tends to enhance the strength of CKD by providing resistance against volume increase of the CKD particle matrix.

The C-S-H sheets in cementitious materials possess interlayer water and between the stacks of C-S-H sheets there exists gel pore water (Wyrzykowski et al. 2017). The redistribution of interlayer and gel pore water occurs during changes in suction (both during drying and wetting). In this process, the C-S-H sheets reorientate to attain equilibrium, tending to reduce the volume of gel pores and leading to the formation of more interlayer pores. This may result in a decrease in the swelling pressure. The additional factors that may contribute to a reduction in swelling pressure are due to the stiffness of the measuring system and an expansion of the specimen ring during a test.

Compressibility parameters and permeability

Figures 9 shows the typical square root of time versus strain plots for the saturated slurried (SS) and compacted CKD specimens (CS-2 kPa, CS-25 kPa and CS-CV) at an applied vertical pressure of 100 kPa. The compression strains were greater in case of specimens SS and CS-2 kPa as compared to that occurred for specimens CS-25 kPa and CS-CV. Higher compression strains of specimens SS and CS-2 kPa are due to the stress history of the specimens during the saturation process. The experimental data at all applied vertical pressures were analysed to determine the changes in the void ratio (Fig. 10), compression index (C_c) (Table 3), swelling index (C_s) (Table 3), coefficient of consolidation (C_v) (Fig. 11), coefficient of volume compressibility (m_v) (Fig. 12), and saturated coefficient of permeability (k) (Fig. 13). The values of C_v, m_v and k were determined based on Terzaghi's consolidation theory. The results of C_v, m_v and k are plotted against the average vertical pressures for two consecutive applied vertical pressures in Figs. 11, 12, and 13 respectively.

The e-log p plots (Fig. 10) show that at any given applied vertical pressure, the void ratio remains in decreasing order magnitude for the specimens SS, CS-2 kPa, CS-25 kPa and CS-CV. The elastic zone for specimens SS and CS-2 kPa remained up to about 25 kPa during the loading stage. A pre-consolidation stress of about 25 kPa for specimen SS possibly originated from the specimen preparation stage. The applied stress for preparing the compacted specimens was far higher (1200 kPa) than that observed as pre-consolidation stress for the compacted specimens.

The applied vertical pressure ranges considered for determining the compression index (C_c) and the swelling index (C_s) are shown in Table 3. The C_c values for all the specimens tested remained between 0.08 and 0.22. Specimen SS exhibited the largest value of C_c, whereas the least value was noted for specimen CS-CV. The void ratio of specimens CS-25 kPa and

CS-CV were very similar prior to the loading stage. Specimen CS-25 kPa exhibited a slightly higher value of C_c as compared to that of specimen CS-CV. The swelling index (C_s) is the slope of the void ratio-vertical pressure plot during unloading or decompression. The C_s values (Table 3) of all specimens tested ranged between 0.007 and 0.019. The lowest value was noted for the specimen CS-CV.

The compression index (C_c) of the CKD was calculated using Skempton's correlation (C_c = 0.007 × (Liquid limit – 10)) and was found to be 0.22. Again, from a relationship with plasticity index (C_c = IP/74, where IP is the plasticity index) (Mitchell 1993), a value of C_c was found to be 0.19. Although these values are close to the value obtained from experimental results for the specimen SS and CS-2kPa, the C_c values of compacted specimens were lower than that were calculated from the correlations considered. Following the relationship C_s = IP/370 (Mitchell 1993), a decompression index of 0.038 was obtained. The experimental C_s values (Table 3) are found to be lesser than that obtained from the correlation.

The Taylor's square-root time fitting method was used to determine the values of C_v for each loading step. The value of C_v depends upon the mineralogy and chemical composition of fine-grained soils. A variation of C_v with an increase in the vertical pressure was noted for all specimens (Fig. 11). The C_v value generally remained between 1 to 10 m^2/year for all the specimens tested and for the pressure ranges considered. A tendency of the specimens to exhibit a C_v value of about 3 m^2/year at high applied pressures can be noted. The C_v values of the CKD (liquid limit = 41%) were found to be similar to that reported for the remoulded soils with liquid limits between 30 and 60% (Lambe and Whitman 1969).

In general, m_v and k decreased with an increase in the applied pressure (Figs. 12 and 13). The m_v and k values were found to be higher for the specimens SS and CS-2 kPa as compared to the specimens CS-25 kPa and CS-CV. Considering the typical m_v values and

descriptive terms of different types of clay reported by Carter (1983), the compressibility of the specimens SS and CS-2 kPa for the range of vertical stress in this study can be described as medium to high, whereas for specimens CS-25kPa and CS-CV, it can be described as low to very low. Results of permeability measurements of different types of CKD have been reported by Todres et al. (1992) on specimens compacted inside permeameter moulds at different densities. The reported values of k were found to be between 1.5×10^{-5} and 1.5×10^{-12} m/s. The k values obtained from one-dimensional oedometer tests in this study (Fig. 13) were within the range of k values reported in the past.

Cyclic freeze-thaw-dry-wet test results

Figure 14a presents the vertical deformation of the CKD specimen with an increasing number of wet-freeze-thaw-dry cycles. The applied temperatures at the top of the specimen during the freezing and drying cycles were -19 and + 52 °C respectively. Therefore, the average temperature gradients along the specimen during freezing and drying cycles were about 0.61 °C/mm and 0.48 °C/mm, respectively. The temperatures at the various salient levels of the specimen during wetting, freezing, thawing and drying cycles are shown in Fig. 14b. The positions of the thermocouples with respect to the top of the specimen (Fig. 6) changed during the test. Therefore, for the sake of consistency in the presentation of the test results, the initial positions of the thermocouples are considered for presenting the temperature data in Fig. 14b. Figure 15 show the temperature profiles along the depth of the specimen at the end of freezing, thawing and drying cycles. As indicated by the readings of the thermocouples (TC0 to TC4 in Figs. 14b and 15), the temperatures measured at various depths of the specimen for the freezing cycles remained higher (less negative) than that of the applied temperature at the top of the specimen. Similarly, the temperatures along the depth of the specimen during the drying cycles were found to be lower than that of the applied temperature at the top of the specimen. The equilibrium temperature profiles along the depth of the specimen can be attributed to the

thermal conductivity and heat capacity of the material, which in turn for the same porous medium, depends upon the volume-mass properties (water content and dry density). Additionally, the heat loss and gain at the base of the specimen and the radial heat loss through the thermal insulation on the exterior mould of the device affected the equilibrium temperature profiles. Tripathy et al. (2017) have reported the effect of temperature gradient, and type and thickness of thermal insulation layer surrounding a testing device on the temperature profiles and moisture distribution in a compacted bentonite. Their results show that the radial heat loss influences the temperature profile and the redistribution of water content within porous media.

The response of the specimens to temperature and hydraulic boundary conditions was reflected on the changes in the height of the specimen in each stage of the tests. Figure 16 shows the measured vertical deformation of the specimen during cycles 1, 3 and 6 for wetting, freezing, thawing and drying processes.

The specimen exhibited very minor swelling deformation (vertical strain less than 0.3%) during the wetting cycles (Figs. 14a and 16a). The swelling deformation decreased with an increasing number of cycles. A lesser swelling deformation of the specimen as compared to that of the specimen CS–2 kPa is attributed to a lower initial compaction dry density of the CKD for this test. The frost heave during the freezing cycles and the thaw settlement during the thawing cycles were found to be of significant magnitudes (Figs. 14a, 16b and c). During the commencements of thawing stages, additional heave was noted. The additional heave is associated with a decrease in effective stress resulting from the increase in pore-water pressure (Eigenbrod 1996).

The partial drying of the specimen during the drying cycles produced vertical deformation that was greater than the swelling deformation but significantly lower than the magnitudes of frost heave and thaw settlement. This resulted in an accumulation of vertical

deformation in the specimen through progressive cycles, causing movement of the top of the sample in an upward direction (i.e., uprising movement) as shown in Fig. 14a. Such a movement pattern has been observed for expansive soils subjected to wet-dry cycles under low surcharge pressures and partial drying conditions (Tripathy et al. 2002). Viklander (1998a) stated that for soils compacted at low dry densities, a net increase in the void ratio occurs upon freeze-thaw processes due to changes in the particle rearrangements.

The strains corresponding to wetting, freezing, thawing and drying were found to be nearly repeatable after four to five cycles (Fig. 14a) indicating that an equilibrium had attained in terms of volume change. The differences in the strains corresponding to the end of freezing cycles and that at the end of a drying cycles was found to be about 42%. At equilibrium, the sum of vertical deformations during wetting and freezing cycles were found to be nearly equal to the sum of vertical deformations occurred during thawing and drying cycles.

The initial compaction conditions are known to influence the engineering properties of geomaterials (Lambe and Whitman 1969). The current study focused on the behaviour of the cement kiln dust at optimum compaction conditions for studying the swelling and compressibility behaviour, and the variation of the permeability. Additionally, the effects of seasonal climatic processes on the volume change behaviour of the cement kiln dust were studied under a low surcharge pressure for which the compaction conditions were on the dry side of the optimum condition. The use of cement kiln dust in various geotechnical and geoenvironmental applications requires developing further understanding of the effects of initial compaction conditions on the volume change, water retention, hydraulic conductivity, and shear strength, both under saturated and unsaturated conditions. Similarly, studies on the behaviour of cement kiln dust upon exposure to various possible sequences of the seasonal climatic processes may enable understanding their long-term behaviour.

Conclusions

One-dimensional swelling and consolidation test results of a cement kiln dust (CKD) for different initial conditions are presented in this paper. The swelling pressure of compacted specimen was measured under constant volume condition. The compressibility parameters (compression index, coefficient of consolidation, and coefficient of volume compressibility) of initially saturated slurried and compacted specimens were studied for an applied pressure range of 2 to 1600 kPa. The values of coefficient of permeability were derived from the results of coefficient of consolidation and coefficient of volume compressibility. A cyclic wetting-freezing-thawing-drying test was conducted on a compacted CKD specimen. The main findings from the laboratory tests on the CKD can be summarised as:

(1) The CKD considered in this study exhibited swelling upon saturation from unsaturated condition. Similarly, swelling pressure developed when an unsaturated specimen was wetted under constant volume condition. The swelling behaviour of the CKD is attributed to the interaction between calcium oxide and water that produce calcium hydroxide.

(2) The applied pressure and initial compaction conditions of CKD influenced the compressibility parameters and the coefficient of permeability. The available correlations between plasticity properties and consolidation parameters for fine grained soils were generally found to overestimate the consolidation parameters of the CKD.

(3) The volume change of the CKD due to repeated wet-freeze-thaw-dry cycles showed strain accumulation. An equilibrium was found to reach after several cycles at which the sum of deformation due to wetting and freezing was similar to the sum of deformation due to thawing and drying.

Data Availability Statement

- Some or all data, models, or code that support the findings of this study are available from the corresponding author upon reasonable request.
- All data, models, and code generated or used during the study appear in the submitted article.
- Some or all data, models, or code generated or used during the study are available in a repository online in accordance with funder data retention policies.

Acknowledgement

This study has been funded by the Engineering and Physical Sciences Research Council (EPSRC) as part of the Climate Adaptation Control Technologies for Urban Spaces (CACTUS) project. For the purpose of open access, the author has applied a creative commons attribution (CC BY) licence to any author accepted manuscript version arising.

References

Adaska, W. H., and D. H Taubert. 2008. "Beneficial uses of cement kiln dust." *In Proceedings of the IEEE/PCA 50th Cement Industry Technical Conference*, Miami, FL, USA, 18–22 May 2008, pp. 210–228. DOI: 10.1109/CITCON.2008.24.

Al-Rawas, A. A, R. Taha, J. D. Nelson, T. B. Al-Shab, and H. Al-Siyabi. 2002. "A comparative evaluation of various additives used in the stabilization of expansive soils." ASTM *Geotech. Test. J.* 25 (2): 199–209. https://doi.org/10.1520/gtj11363j.

ASTM. 2010. *Standard test method for shrinkage factors of soils by the wax method.* ASTM D4943-08, West Conshohocken, PA.

ASTM. 2015. *Standard Guide for Commercial Use of Lime Kiln Dusts and Portland Cement Kiln Dusts.* ASTM D5050-08, West Conshohocken, PA.

Baghdadi, Z. A., and M. A. Rahman. 1990. "The potential of cement kiln dust for the stabilization of dune sand in highway construction." *Build. and Environ.* 25 (4): 285–289. https://doi.org/10.1016/0360-1323(90)90001-8.

Baghdadi, Z. A., M. N. Fatani, and N. A. Sabban. 1995. "Soil modification by cement kiln dust." *J. of Mater. in Civil Eng.* 7(4): 218–222. https://doi.org/10.1061/(ASCE)0899-1561(1995)7:4(218).

Bhatty, J. I., S. Bhattacharja, and H. A. Todres. 1996. "Use of cement kiln dust in stabilizing clay soils." Portland Cement Association, PCA Serial No. 2035, Skokie, Illinois, USA. https://doi.org/10.1061/40744(154)10.

BS 1377. 1990a. *Methods of test for Soils for civil engineering purposes.* BS 1377 Part 2 – Classification tests, BSI, London UK.

BS 1377. 1990b. *Methods of test for Soils for civil engineering purposes.* BS 1377 Part 4 - Compaction-related tests, BSI, London UK.

BS 1377. 1990c. *Methods of test for Soils for civil engineering purposes.* BS 1377 Part 5 - Compressibility, permeability and durability tests, BSI, London, UK.

Button, J. W. 2003. "Kiln Dust for Stabilization of Pavement Base and Subgrade Materials." *Report No. TTI2003-1, Texas Transportation Institute, College Station, Texas, USA.*

Carter, M. 1983. *Geotechnical engineering handbook.* Pentech Press Limited, London.

Chamberlain, E. J., and A. J. Gow. 1979. Effect of freezing and thawing on the permeability and structure of soils. *Eng. Geol.* 13(1–4): 73–92. https://doi.org/10.1016/0013-7952(79)90022-X.

Department for Business and Trade. 2023. *Unlocking Resource Efficiency Phase 1 Cement and Concrete Report*. DESNZ Research Paper Series Number 2023/039. https://www.gov.uk/government/publications/unlocking-resource-efficiency.

Dyer, T. D., J. E., Halliday, and R. K. Dhir. 1999. "An investigation of the hydration chemistry of ternary blends containing cement kiln dust." *J. of Mater. Sc.* 34: 4975-4983. https://doi.org/10.1023/A:1004715806829.

Eigenbrod K. D. 1996. "Effects of cyclic freezing and thawing on volume changes and permeabilities of soft fine-gained soils." *Can. Geotech. J.* 33(4): 529–537.

Eltantawy I. M, and P. W. Arnold. 1973. "Reappraisal of ethylene glycol mono-ethyl ether (EGME) method for surface area estimation of clays." *J. Soil Sc.* 24: 232-238. https://doi.org/10.1111/j.1365-2389.1973.tb00759.x.

Environment Agency. 2021. *Waste Classification — Guidance on the classification and assessment of waste Technical Guidance WM3*. Natural Resources Wales, Scottish Environment Protection Agency (SEPA), Northern Ireland Environment Agency (NIEA), Environment Agency. https://www.gov.uk/government/publications/waste-classification-technical-guidance.

Heincke, S., J. Maksimainen, and S. Reiter. 2023. “Decarbonising cement and concrete value chains: Takeaways from Davos (Part 1).” *World Cement Special Report*, 06 February 2023, David Bizley (Ed.). https://www.worldcement.com/special-reports/06022023/decarbonizing-cement-and-concrete-value-chains-takeaways-from-davos-part-1/.

Hui, B., and H. Ping. 2009. “Frost heave and dry density changes during cyclic freeze-thaw of a silty clay.” *Permafrost and periglacial Processes* 20(1): 65–70. https://doi.org/10.1002/ppp.636.

Konrad, J-M. 1989. “Effect of freeze–thaw cycles on the freezing characteristics of a clayey silt at various overconsolidation ratios.” *Can. Geotech. J.* 26(2): 217–226. https://doi.org/10.1139/t89-031.

Kunal, P., R. Siddique, and A. Rajor. 2012. “Use of cement kiln dust in cement concrete and its leachate characteristics.” *Resources, Conservation and Recycling* 61: 59–68. https://doi.org/10.1016/j.resconrec.2012.01.006.

Lambe, T. W. and R. V. Whitman. 1969. *Soil Mechanics*. John Wiley, New York.

Lavkulich, L. M. 1981. *Methods manual: Pedology Laboratory*. Department of Soil Science, University of British Columbia, Vancouver, BC.

Liyanage, J., and R. P. Gamage. 2021. “The hydration and volume expansion mechanisms of modified expansive cements for sustainable In-Situ Rock Fragmentation: A Review.” *Energies* 14, 5965. https://doi.org/10.3390/en14185965.

Mackie, A., S. Boilard, M. E. Walsh, and C. B. Lake. 2010. “Physicochemical characterization of cement kiln dust for potential reuse in acidic wastewater treatment.” *J. Hazard. Mater.* 173 (1-3): 283-291. https://doi.org/10.1016/j.jhazmat.2009.08.081.

Miller, G. A., and S. Azad. 2000. “Influence of soil type on stabilization with cement kiln dust.” *Const. and Build. Mater.* 14 (2): 89–97. https://doi.org/10.1016/S0950-0618(00)00007-6.

Miller, G. A, S. Azad, and B. Dhar. 1997. “The effect of cement kiln dust on the collapse potential of compacted shale.” *Testing Soil Mixed with Waste or Recycled Materials*, Wasemiller MA and Hoddinott KB (editors), ASTM Committee D-18 on Soil and Rock.; ASTM International, West Conshohocken, Pa.: ASTM International; 1997: 232–245.

Mitchell, J. K. 1993. *Fundamentals of soil behaviour*. 2nd ed. New York; Chichester: John Wiley & Sons.

Parsons, R. L., E. Kneebone, and J. P. Milburn. (2004). “Use of cement kiln dust for subgrade stabilization.” Final Report No. KS-04-03, Kansas Department of Transportation, Topeka, Kansas.

Peethamparan, S., J. Olek., and J. Lovell. 2008. “Influence of chemical and physical characteristics of cement kiln dusts (CKDs) on their hydration behavior and potential suitability for soil stabilization.” *Cement and Conc. Res.* 38: 803–815. https://doi.org/10.1016/j.cemconres.2008.01.011.

Prakash, K., and A. Sridharan. 2009. “Beneficial Properties of Coal Ashes and Effective Solid Waste Management.” Practice Periodical of Hazardous, Toxic, and Radioactive Waste Management. 13(4): 217-294. https://doi.org/10.1061/(ASCE)HZ.1944-8376.0000014.

Qi, J., W. Ma., and Song, C. 2008. “Influence of freeze-thaw on engineering properties of a silty soil.” *Cold Reg. Sc. Tech.* 53(3): 397–404. https://doi.org/10.1016/j.coldregions.2007.05.010.

Ramachandran, V. S., P. J. Sereda., and R. F. Fieldman. 1964. “Mechanism of hydration of calcium oxide.” *Nature* 201: 288-289. https://doi.org/10.1038/201288a0.

Ravindrarajah, R. S. 1982. “Usage of cement kiln dust in concrete.” *Int. J. Cement Composites and Lightweight Conc.* 4(2): 95-102. https://doi.org/10.1016/0262-5075(82)90013-6.

Sreekrishnavilasam, A. and M. C. Santagata. 2006. “Development of Criteria for the Utilization of Cement Kiln Dust (CKD) in Highway Infrastructures.” Report No. FHWA/IN/JTRP-2005/10, Joint Transportation Research Program, Indiana Department of Transportation and Purdue University, West Lafayette, Indiana, USA, https://doi.org/10.5703/1288284313395.

Todres, H. A., A. Mishulovich, and J. Ahmed. 1992. *Cement kiln dust management: Permeability*. Research and Development Bulletin RD 103T, Portland Cement Association, Skokie, Ill., pp. 1–6.

Tripathy, S., O. M. Al-Hussaini, P. J. Cleall, S. W. Rees, and H. Wang. 2020. “Frost heave and thaw settlement of initially saturated-slurried and compacted-saturated materials.” *E3S Web of Conference* 195 03036. https://doi.org/10.1051/e3sconf/202019503036.

Tripathy, S., H. R. Thomas, and P. Stratos. 2017. “Response of Compacted Bentonites to Thermal and Thermo-Hydraulic Loadings at High Temperatures.” *Geosciences* 7(3), https://doi.org/10.3390/geosciences7030053.

Tripathy, S., K. S. Subba Rao, and D. G. Fredlund. 2002. “Water content - void ratio swell shrink paths of compacted expansive soils.” *Can. Geotech. J.* 959: 938–959. https://doi.org/10.1139/t02-022.

USEPA. 1998. “Technical Background Document on Ground Water Controls at CKD Landfills.” *Office of Solid Waste U.S. Environmental Protection Agency* (USEPA), Washington, D.C., USA.

Viklander, P. 1998a. “Laboratory study of stone heave in till exposed to freezing and thawing.” *Cold Reg. Sc. Tech.* 27(2): 141–152. https://doi.org/10.1016/S0165-232X(98)00004-4.

Viklander, P. 1998b. “Permeability and volume changes in till due to cyclic freeze/thaw.” *Can. Geotech. J.* 35(3): 471–477. https://doi.org/10.1139/t98-015.

Wang, S-l, Q-f, Lv., H. Baaj, X-y. Li, and Y-x, Zhao. 2016. “Volume change behaviour and microstructure of stabilized loess under cyclic freeze–thaw conditions.” *Can. J. Civil Eng.* 43 (10): 865–874. https://doi.org/10.1139/cjce-2016-005.

Wyrzykowski, M., P. J. McDonald, K. L. Scrivener, and P. Lura. 2017. “Water Redistribution within the Microstructure of Cementitious Materials due to Temperature Changes Studied with ^{1}H NMR.” *J. Phys. Chem. C*, 121: 27950–27962. https://doi.org/10.1021/acs.jpcc.7b08141.

Table1. Properties of the cement kiln dust used in this study

Specific gravity, G_s[1]	2.72
Atterberg limits	
Liquid limit, LL (%)[2]	41
Plastic limit, PL (%)	27
Plasticity index, PI (%)	14
Shrinkage limit, SL (%)[3]	21
Particle size distribution[4]	
Sand (%)	….
Silt-size (%)	71
Clay-size (%)	29
Compaction characteristics[5]	
Optimum water content (%)	27.6
Maximum dry unit weight (kN/m^3)	14.85
Cation exchange capacity (CEC), (meq/100g)[6]	
Na^+	3.22
Ca^{2+}	60.12
Mg^{2+}	2.41
K^+	13.46
Total Cation Exchange Capacity (meq/100g)	79.21
Specific surface area (m^2/g)[7]	0.58

[1, 2, 4, 5] BS 1377 (1990); [3] ASTM D4943 (2010); [6] Ammonium acetate method at pH 7 (Lavkulich 1981); [7] Ethylene Glycol Monoethyl Ether (EGME) method (Eltantawy and Arnold 1973)

Table 2. Chemical composition of the CKD used in this study

Oxides	%
SiO_2	13.02
Al_2O_3	2.65
Fe_2O_3	1.04
CaO	41.46
K_2O	1.33
Na_2O	0.21
MgO	1.07
SO_3	1.84
SrO	0.04
P_2O_5	0.05
Mn_2O_3	0.06
TiO_2	0.14
ZnO	0.01
Cr_2O_3	0.01
LOI	33.8
pH	12.07

Table 3. Compression and swell indices of the cement kiln dust specimens tested

Description of specimen prior to loading/unloading	Vertical stress range for determining C_c and C_s (kPa - kPa)	Compression index, C_c	Swelling index, C_s
Saturated-slurried (SS)	25 - 800	0.22	0.019
Saturated at an applied pressure of 2 kPa (CS – 2 kPa)	14 - 1602	0.18	0.018
Saturated at an applied pressure of 25 kPa (CS – 25 kPa)	125 -1625	0.10	0.017
Saturated under constant volume condition (CS – CV)	100 - 1600	0.08	0.007

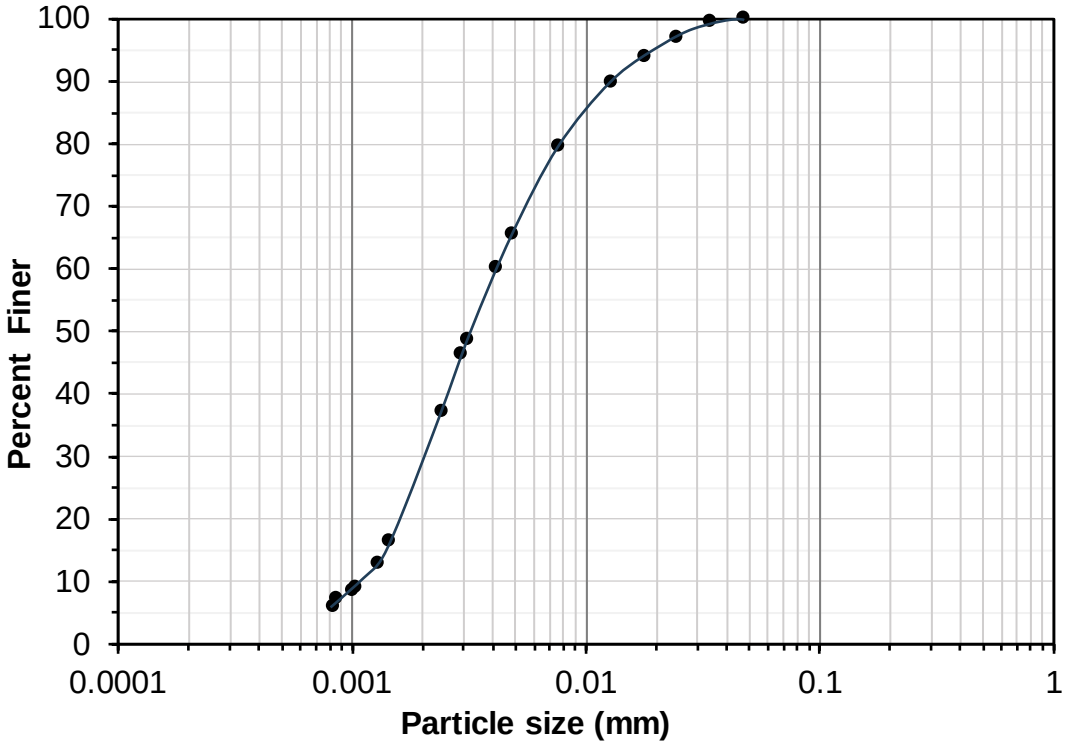

Fig. 1. Grain-size distribution curve of the cement kiln dust used.

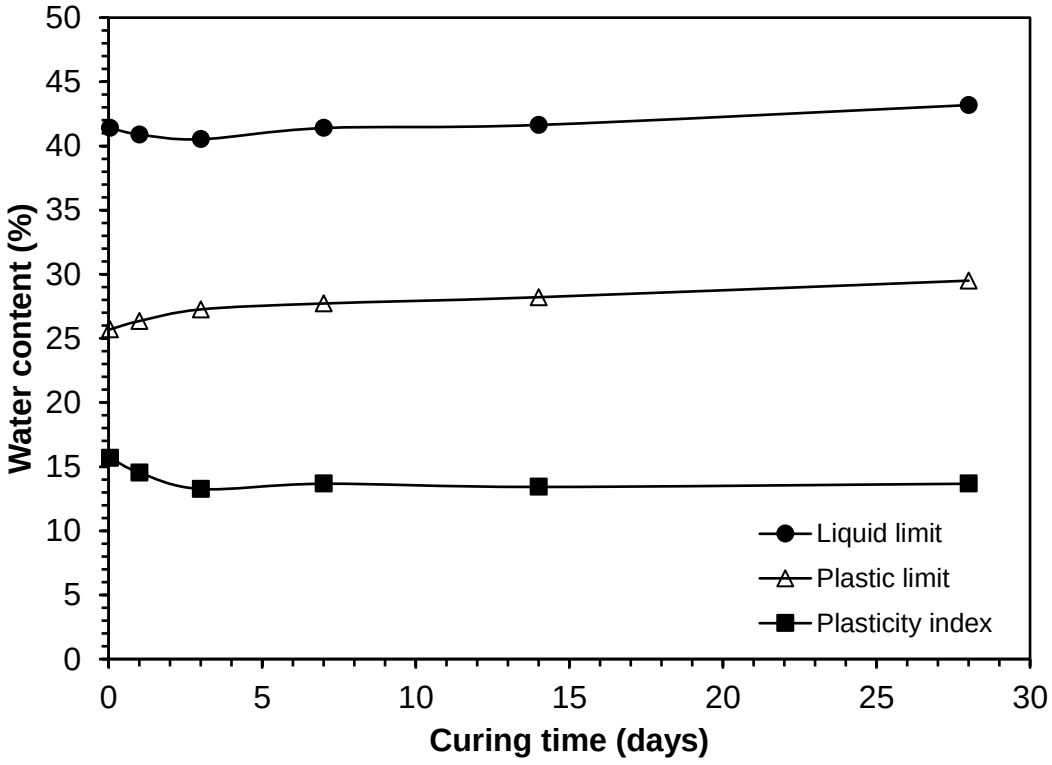

Fig. 2. Effect of curing time on liquid and plastic limits of the CKD used in this study.

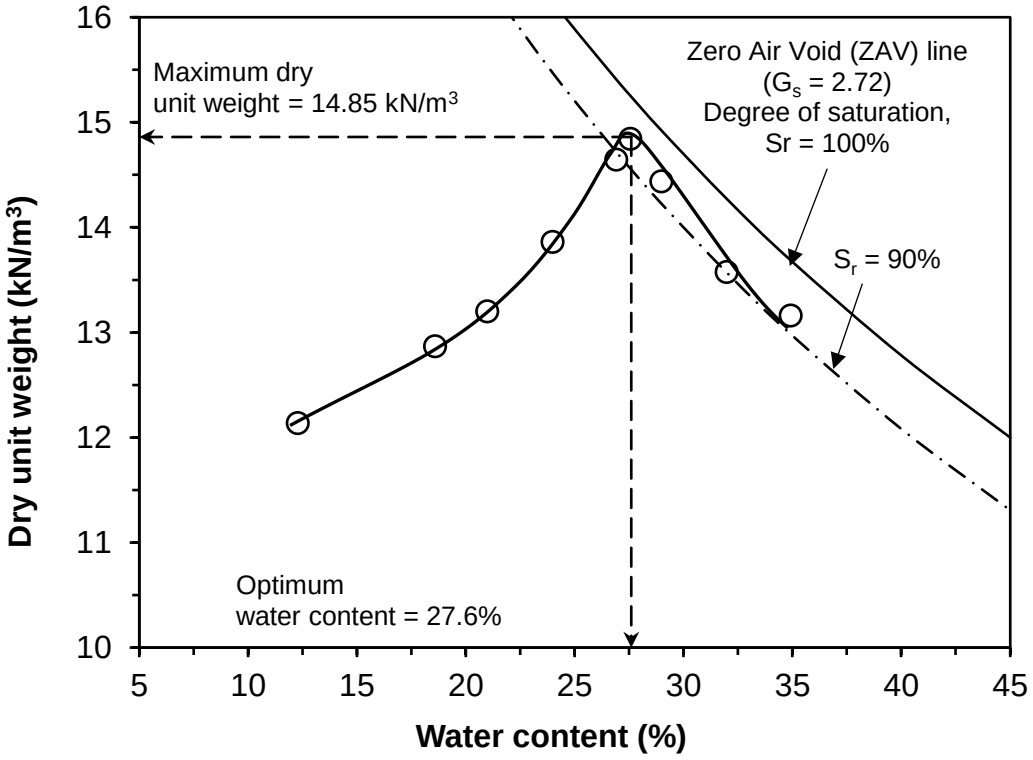

Fig. 3. Light compaction curve of the cement kiln dust used.

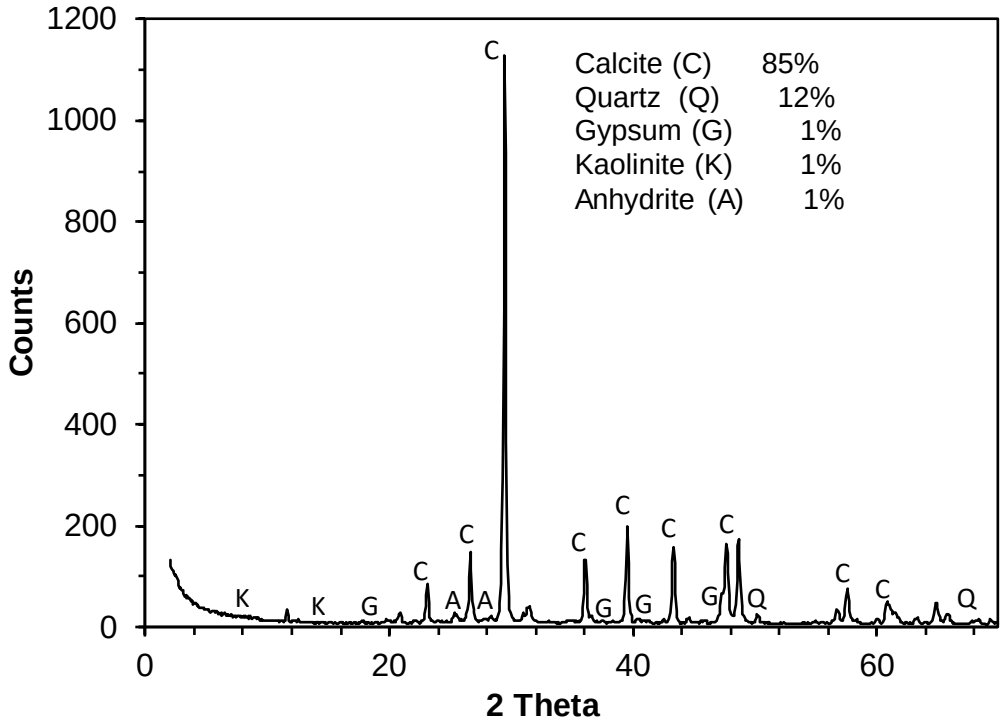

Fig. 4. X-ray diffraction spectra of the CKD used in this study.

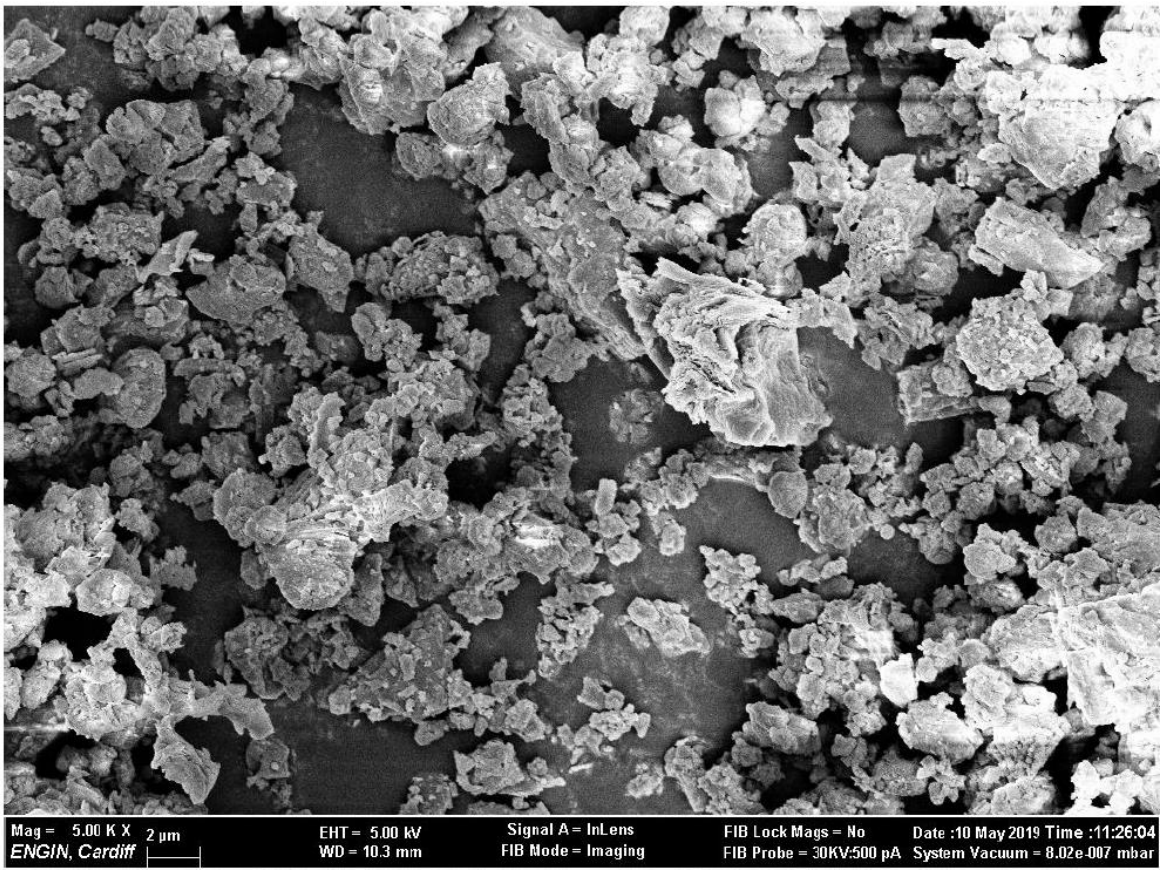

Fig. 5. Scanning electron photomicrograph of the CKD.

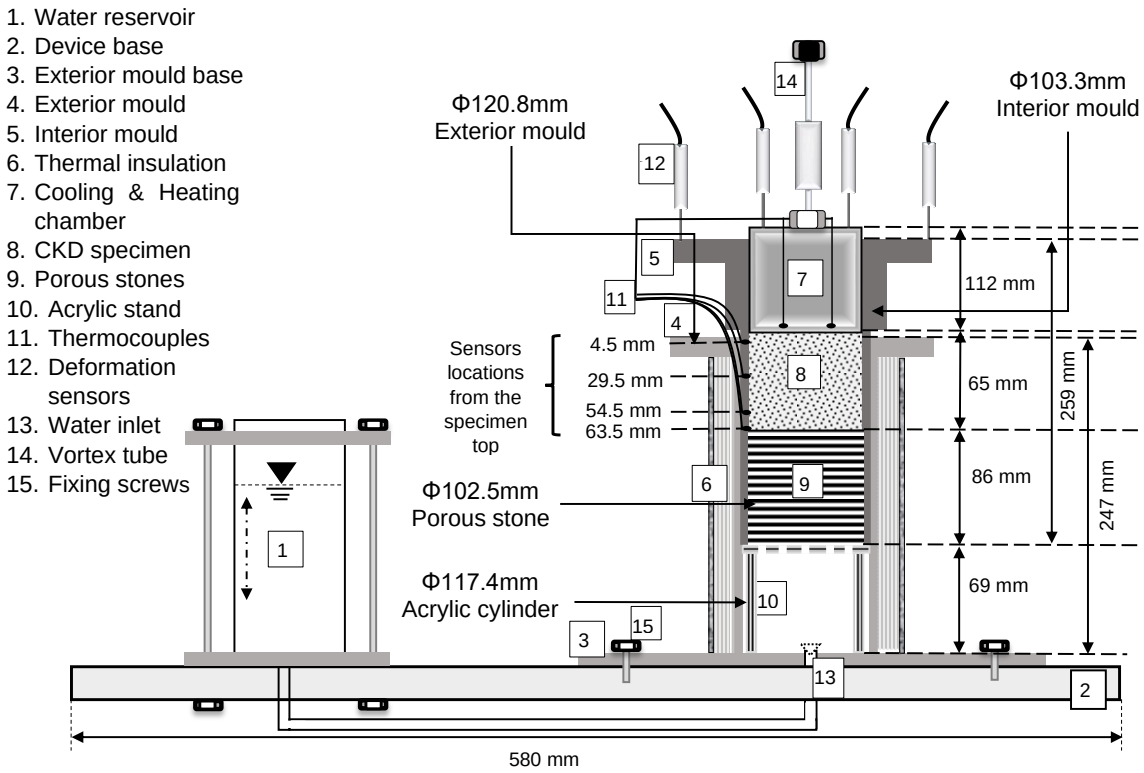

Fig. 6. A schematic of the test set up for cyclic wet-freeze-thaw-dry test.

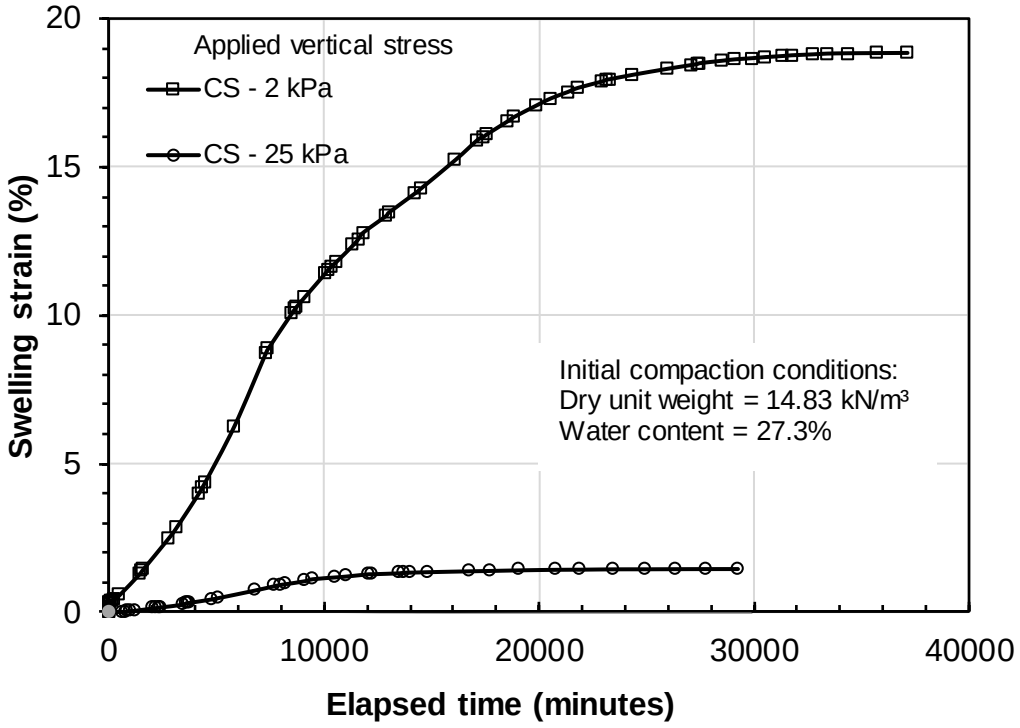

Fig. 7. One-dimensional swelling strain of compacted CKD specimens at the selected applied vertical pressures in this study.

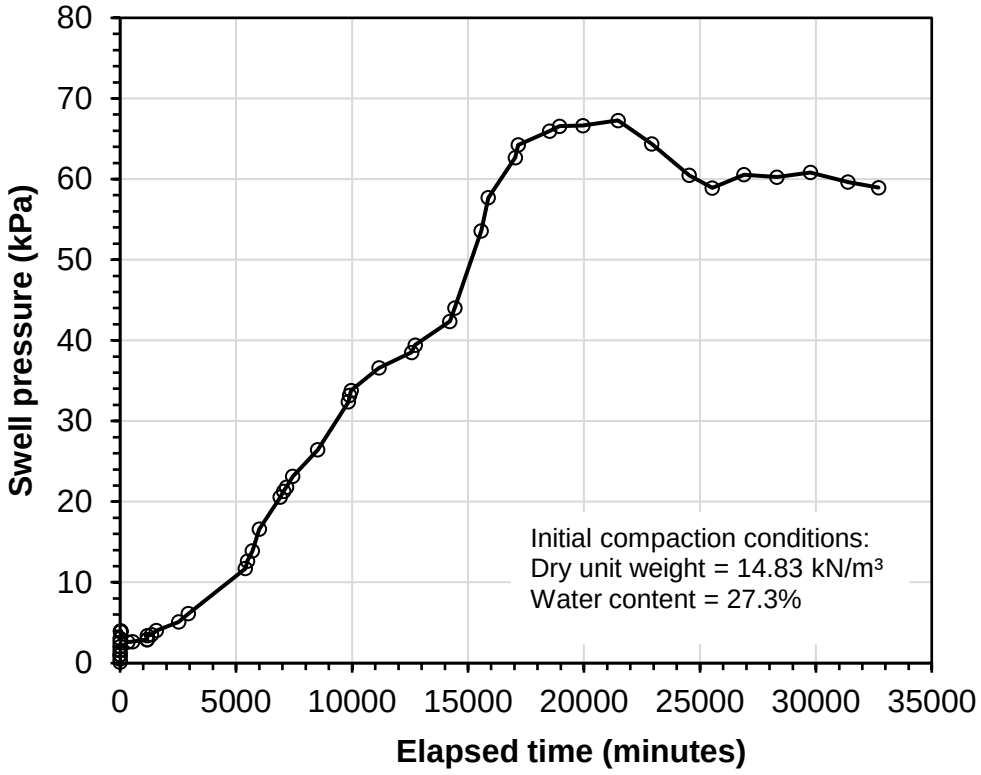

Fig. 8. Constant volume-swelling pressure test results of a compacted CKD specimen.

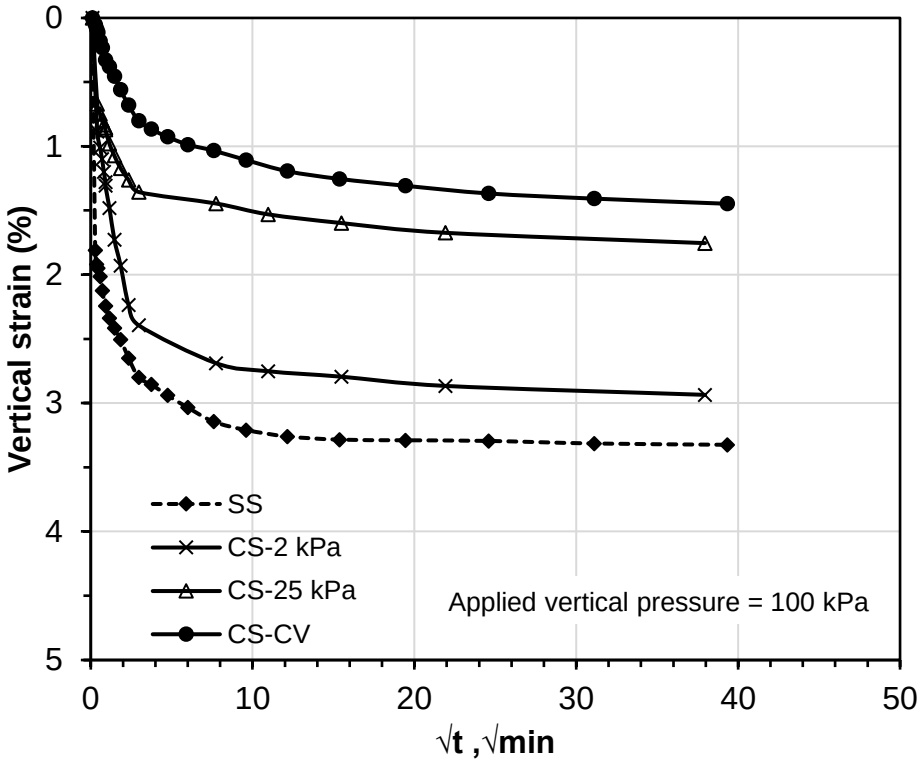

Fig. 9. Typical time-compression plots of CKD specimens at an applied vertical pressure of 100 kPa.

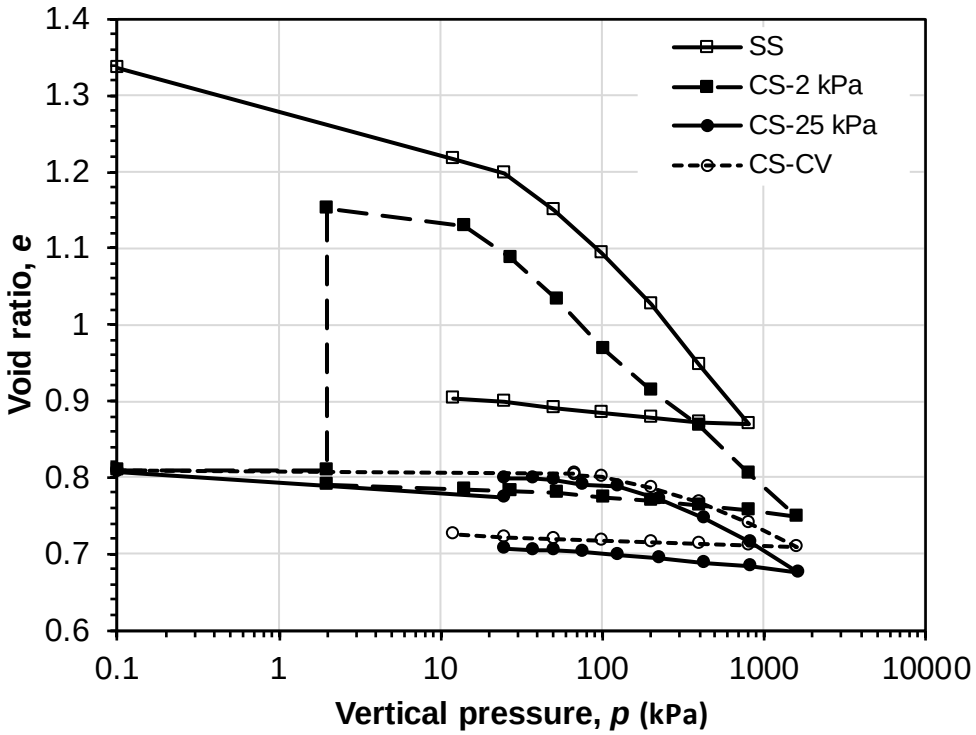

Fig. 10. *e*-log *p* plots of saturated slurried and compacted-saturated cement kiln dust specimens.

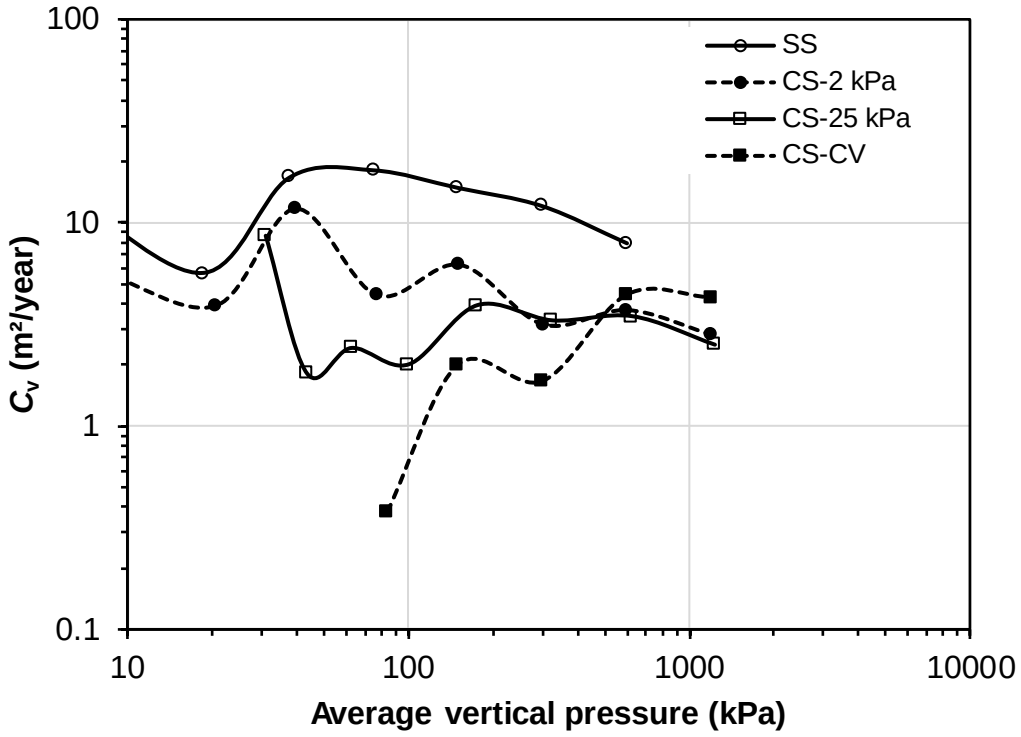

Fig. 11. Effect of vertical pressure on the coefficient of consolidation of the CKD.

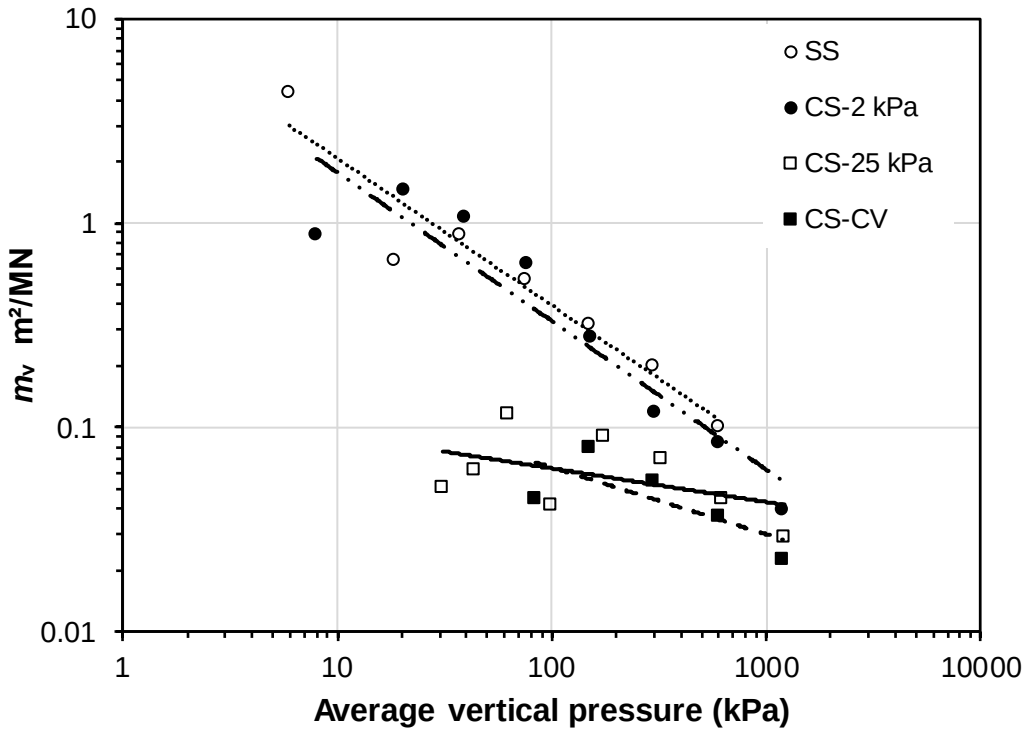

Fig. 12. Effect of vertical pressure on the coefficient of volume compressibility of the CKD.

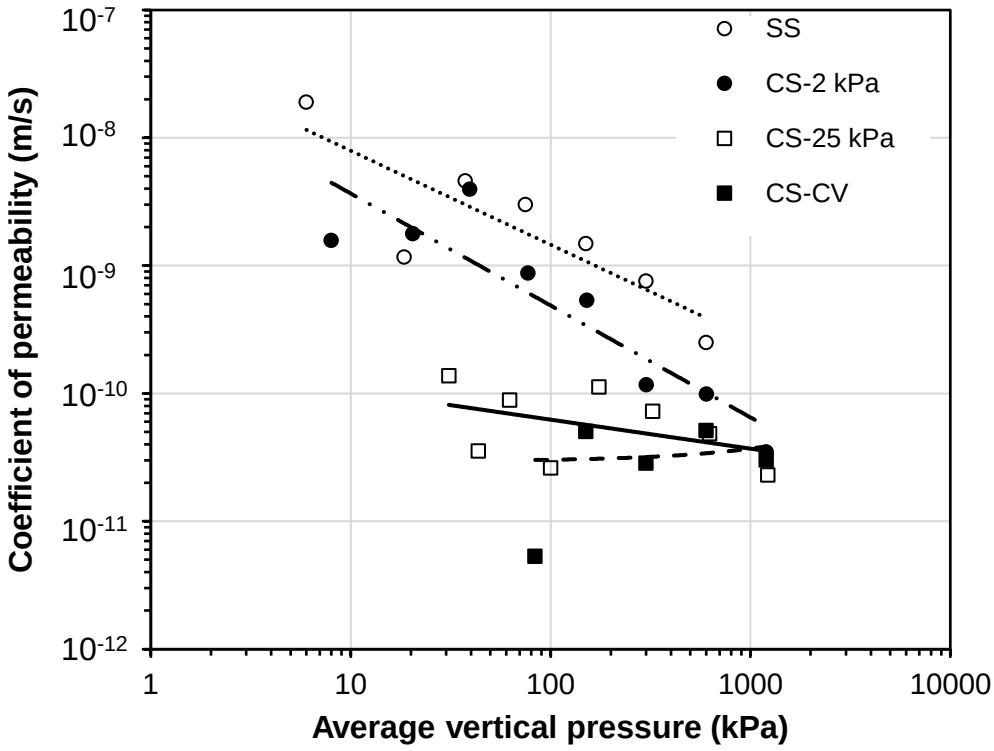

Fig. 13. Coefficient of permeability of the CKD.

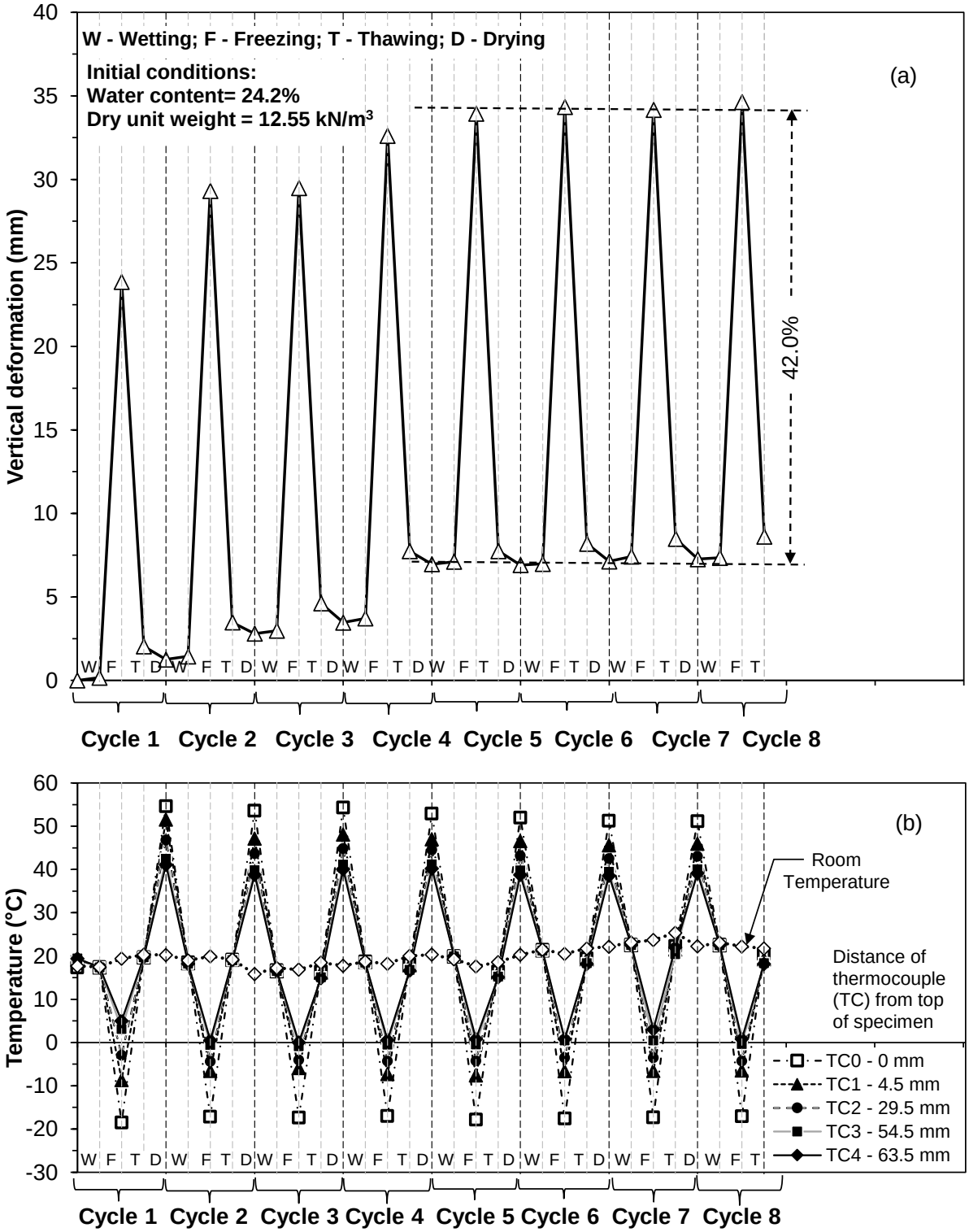

Fig. 14. Cyclic wet-freeze-thaw-dry test results, (a) vertical deformation and (b) temperature.

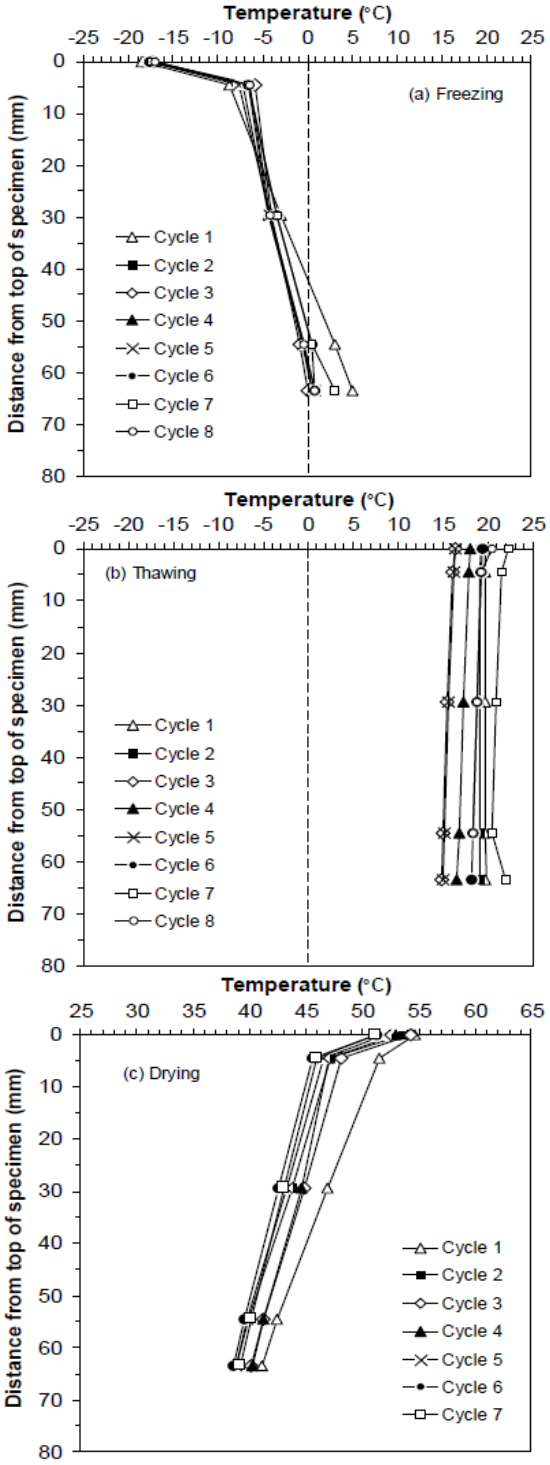

Fig. 15. Temperature profiles at the end of (a) freezing, (b) thawing and (c) drying cycles.

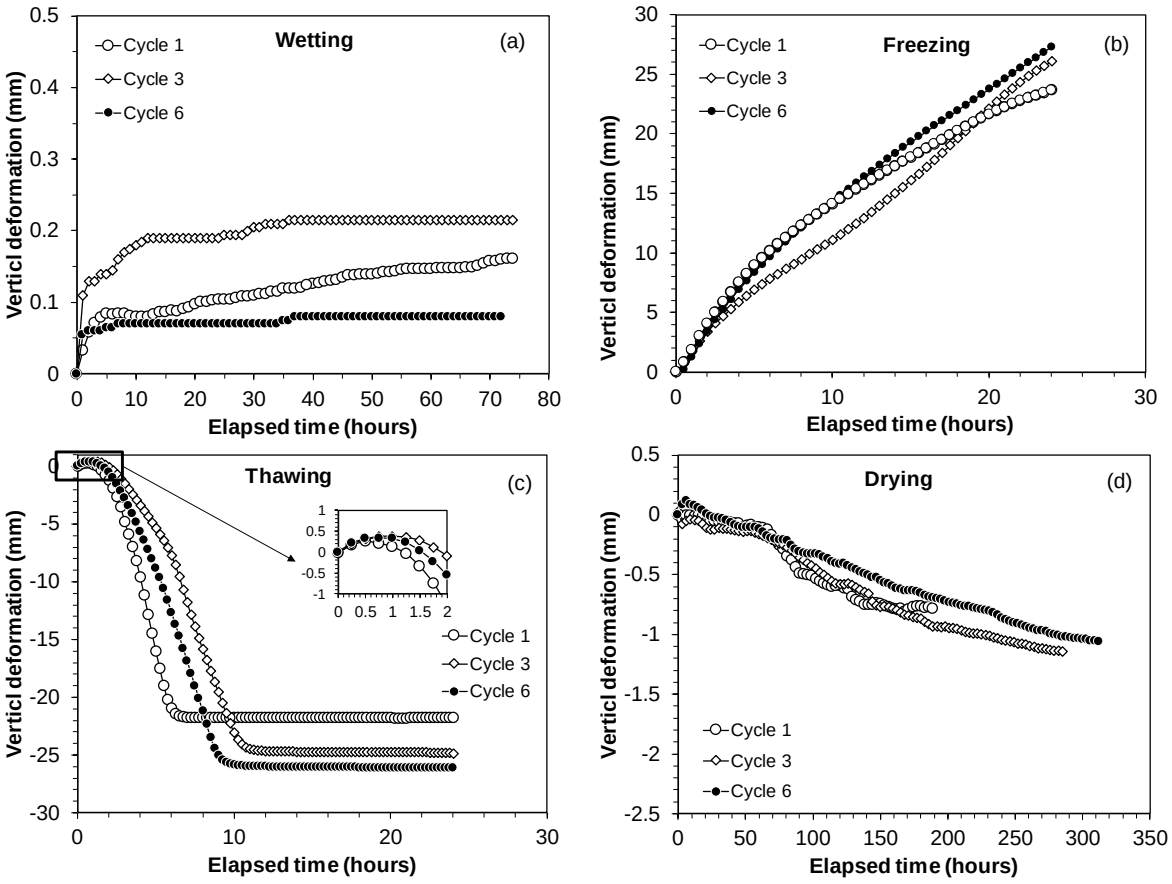

Fig. 16. Vertical deformation of the CKD specimen during cycles 1, 3, and 6; (a) wetting, (b) freezing, (c) thawing, and (d) drying.